Isı Bilimi ve Tekniği Dergisi, 35, 2, 75-88, 2015
J. of Thermal Science and Technology

ISSN 1300-3615

DEVISED APPLICATION OF LABVIEW FOR AN AUTOMATIC TEST SYSTEM BASED ON GENERATION, CONTROL AND PROCESSING OF PULSATILE PIPE FLOWS

Emrah ÖZAHİ* and Melda Özdinç ÇARPINLIOĞLU**
*University of Gaziantep Faculty of Engineering Mechanical Engineering Department
27310 Şehitkamil, Gaziantep, ozahi@gantep.edu.tr
**University of Gaziantep Faculty of Engineering Mechanical Engineering Department
27310 Şehitkamil, Gaziantep, melda@gantep.edu.tr

(Geliş Tarihi: 28.05.2014, Kabul Tarihi: 27.03.2015)

Abstract: This paper presents an automated generation, control, data acquisition and processing of sinusoidal pulsatile pipe flow using a devised program in LabView 2009SP1® in the experimental ranges of the time-averaged Reynolds number, Re_{ta} of $1019\pm35\leq Re_{ta}\leq 4817\pm164$, the oscillating Reynolds number, Re_{os} of $107\pm4\leq Re_{os}\leq 4261\pm145$, the velocity amplitude ratio, A_1 of $0.05\pm0.0017\leq A_1\leq 0.96\pm0.03$ and the Womersley number, $\sqrt{\omega'}$ of $2.72\pm0.00\leq\sqrt{\omega'}\leq 32.21\pm0.00$. The aim herein is to introduce the devised program named as *Time Dependent Flow Control.vi* (*TDFC.vi*) within the methodology developed for pulsatile pipe flow analyses. The program provides a considerable contributions for both education and specific research studies. It has also been designed to minimize workload of an engineer and to improve the efficiency and accuracy of the system. The proposed program leads further experimental studies related on steady and time dependent flow dynamics. The experimental results are given to show the functionality of the system for the real-world data acquisition with great accuracy. As a result, the devised program in LabView 2009SP1® (*TDFC.vi*) provides more accurate and feasible velocity and frictional field analyses in pulsatile pipe flows when compared with the conventional analyzing methods, especially in transition to turbulent regime, with an acceptable error margin eliminating any possible human error.
Keywords: Labview, Automatic test system, Automated control and measurement, Pulsatile flow control, Data acquisition.

DARBELİ BORU AKIŞLARININ ÜRETİMİ, KONTROLÜ VE İŞLENMESİNE DAYALI OTOMATİK BİR TEST SİSTEMİ İÇİN LABVIEW PROGRAMINDA GELİŞTİRİLEN BİR UYGULAMA

Özet: Bu makale, zaman ortalamalı Reynolds sayısı $1019\pm35\leq Re_{ta}\leq 4817\pm164$, salınım Reynolds sayısı, $107\pm4\leq Re_{os}\leq 4261\pm145$, hız genlik oranı, $0.05\pm0.0017\leq A_1\leq 0.96\pm0.03$ ve Womersley sayısı, $2.72\pm0.00\leq\sqrt{\omega'}\leq 32.21\pm0.00$ deney aralıklarında, LabView 2009SP1® yazılım programında geliştirilmiş bir program kullanarak, sinüsel darbeli boru akışının otomatikleştirilmiş üretimi, kontrolü, veri toplama ve işlenmesini sunmaktadır. Burada ki amaç, içerisinde darbeli boru akışı analizleri için geliştirilmiş yöntem bilimini barındıran *Time Dependent Flow Control.vi* (*TDFC.vi*) ismi ile oluşturulan programı tanıtmaktır. Geliştirilen program hem eğitim hem de belirli araştırma çalışmaları için önemli katkılar sağlamaktadır. Program ayrıca mühendislik iş yükünü minimum seviyeye indirmek ve sistemin verimliliğini ve doğruluğunu artırmak için tasarlanmıştır. Geliştirilen program zamana bağımsız ve bağımlı akım dinamikleri ile ilgili gelecekteki deneysel çalışmalar için yol göstermektedir. Deneysel sonuçlar gerçek verilerin toplanmasında mükemmel doğruluklarla sistemin işlevselliğini göstermek için verilmiştir. Sonuç olarak, LabView 2009SP1® (*TDFC.vi*) de oluşturulan program, darbeli boru akışlarında, özelliklede türbülansa geçiş rejiminde, geleneksel analiz etme yöntemleri ile kıyaslandığında, muhtemel insan hatasını ortadan kaldırarak daha hassas ve elverişli hız ve sürtünme alanı analizleri sağlamaktadır.
Anahtar Kelimeler: LabView, Otomatik test sistemi, Otomatikleştirilmiş kontrol ve ölçüm, Darbeli akış kontrolü, Veri toplama.

NOMENCLATURE

A_1	velocity amplitude ratio $[=\lvert\overline{U}_{m,os,1}\rvert/\overline{U}_{m,ta}]$
D	pipe inner diameter [m]
f	frequency of oscillation [Hz]
L	pipe length through which the pressure gradient [m]
$M_0(\sqrt{\omega'})$	modulus of the first kind Bessel function of zeroth order, $J_0(i^{3/2}\sqrt{\omega'})$
$P(t)$	instantaneous pressure [Pa]
$\overline{P}_{ta}$	time averaged component of ensemble averaged pressure [Pa]
$\lvert\overline{P}_{os}\rvert$	amplitude of ensemble averaged pressure [Pa]
r	radial position from centerline [m]
R	pipe radius [m]
Re_{os}	oscillating Reynolds number $[=\lvert\overline{U}_{m,os,1}\rvert D/\nu]$

Re_{ta} time-averaged Reynolds number $[=\overline{U}_{m,ta}D/\nu]$

Re_{δ_S} Reynolds number based on the Stokes-layer thickness $[=|\overline{U}_{m,os,1}|\delta_S/\nu]$

Q volumetric flow rate [m^3/s] $[=2\pi\int_0^R u(r)rdr]$

S stokes parameter $[=R\sqrt{\omega/2\nu}]$

t time coordinate [s]

T oscillation period [s]

u characteristic velocity [m/s]

$U(r,t)$ instantaneous axial velocity [m/s]

$\overline{U}(t)$ ensemble-averaged value of instantaneous velocity [m/s]

$\overline{U}_{ta}$ time-averaged component of local velocity at any radial position of the probe [m/s]

$|\overline{U}_{os,1}|$ oscillating component of local velocity at any radial position of the probe [m/s]

$\overline{U}_m(t)$ instantaneous mean velocity [m/s]

$|\overline{U}_{m,os,1}|$ oscillating component of cross-sectional mean velocity [m/s]

$\overline{U}_{m,ta}$ time-averaged component of cross-sectional mean velocity [m/s]

X axial length from the end of MFC unit [m]

Greek Letters

∂ partial derivative

δ_S Stokes-layer thickness [m] $[=\sqrt{2\nu/\omega}]$

$\Delta\overline{P}(t)/L$ instantaneous pressure drop per unit length [Pa/m]

$\lambda_u(t)$ instantaneous friction factor

$\lambda_{u,ta}$ time averaged friction factor

λ_{qL} instantaneous laminar quasi-steady friction factor

ν kinematic viscosity [m^2/s]

ω angular frequency of oscillation $[=2\pi f]$ [rad/s]

ω' dimensionless frequency of oscillation $[=R^2\omega/\nu]$

$\sqrt{\omega'}$ Womersley number, $[=R\sqrt{\omega/\nu}]$

ρ fluid density [kg/m^3]

$\theta_0(\sqrt{\omega'})$ phase of the first kind Bessel function of zeroth order, $J_0(i^{3/2}\sqrt{\omega'})$

$\overline{\tau}_\omega(t)$ instantaneous wall shear stress [Pa]

Abbreviates

FFT fast Fourier transformation

MFC mass flow control

RMS root mean square

subvi sub virtual instrument

TDFC time dependent flow control

TDP turbulence detection parameter

TP threshold parameter

vi virtual instrument in LabView

Others

$\angle$ phase lag

INTRODUCTION

One of fundamental patterns in time dependent flows is pulsatile one in which flow is composed of a steady component and a superimposed periodical time varying component called oscillation. Flow dynamics analysis in pulsatile flow is more difficult when compared with that in steady flows. Therefore, there is a need to devise a fully-automated program in any software interface to generate, process and analyze such types of flows. There are many attempts for investigation of flow dynamics in pulsatile pipe flows. In the study of Ohmi et al. (1982), the flow pattern for pulsatile laminar pipe flow was researched and classified into three types as quasi-steady, intermediate and inertia dominant regions with respect to the dimensionless frequency parameter, Womersley number, $\sqrt{\omega'}$. There are very few studies in which cross sectional velocity profiles are investigated. Mizushina et al. (1973) studied the effect of $\sqrt{\omega'}$ on the shapes of velocity profiles. On the other hand, Ohmi and Iguchi (1981) studied on the frictional field in time dependent pipe flows. As a result of the literature survey, it can be said that the relevant literature are mainly based on observations of velocity waveforms and detection of disturbance growth. To perform velocity and frictional field analyses in details, a devised automated software program is necessary in order to eliminate any potential human errors.

There is no fully-automated program devised in LabView environment for time dependent flow generation, control, data acquisition and processing up to now. The program named as *Time Dependent Flow Control.vi*, *TDFC.vi* is constructed for this purpose. Before introducing the utilized program within the used methodology, it is needed to handle the basic terminology of pulsatile pipe flow dynamics which are used in the program. In time dependent pipe flows, the instantaneous mean velocity, $\overline{U}_m(t)$ profiles are evaluated by numerically integrating the ensemble averaged data over the pipe cross section by means of the well-known Sympson's rule. The evaluated values of $\overline{U}_m(t)$ are then approximated by the first harmonics of the sine wave using the following finite Fourier series expansion;

$$\overline{U}_m(t)=\overline{U}_{m,ta}+|\overline{U}_{m,os,1}|\sin(\omega t+\angle\overline{U}_{m,os,1}) \quad (1)$$

Similarly, the time averaged component of ensemble averaged pressure, $\overline{P}_{ta}$ and the amplitude, $|\overline{P}_{os}|$ are presented by the first harmonics of the sine wave using the Eq. (2);

$$\overline{P}=\overline{P}_{ta}+|\overline{P}_{os,1}|\sin(\omega t+\angle\overline{P}_{os,1}) \quad (2)$$

The values of the instantaneous wall shear stress, $\overline{\tau}_\omega(t)$, for different phases of the cycle are then evaluated by substituting the evaluated values of the instantaneous pressure drop per unit length, $\Delta\overline{P}(t)/L$ and $d\overline{U}_m(t)/dt$ into the following time dependent momentum integral equation;

$$\rho \frac{d\overline{U}_m(t)}{dt} + \frac{4\overline{\tau}_w(t)}{D} = \frac{\Delta\overline{P}(t)}{L} \quad (3)$$

The instantaneous friction factor, $\lambda_u(t)$, and the time averaged friction factor, $\lambda_{u,ta}$, are evaluated using the following definitions given in the literature (Ohmi and Iguchi, 1980);

$$\lambda_u(t) = 8\overline{\tau}_w(t) \Big/ \rho \overline{U}_m{}^2(t) \quad (4)$$

$$\lambda_{u,ta} = \frac{8}{\rho \overline{U}_{m,ta}^3 T} \int_0^T \overline{\tau}_w(t)\overline{U}_m(t)dt \quad (5)$$

Instantaneous laminar quasi-steady friction factor, λ_{qL} is also calculated as follows;

$$\lambda_{qL}(t) = 64\nu \big/ \overline{U}_m(t)D \quad (6)$$

The details of the basic terminology of the pulsatile pipe flows can also be found in (Gündoğdu and Çarpınlıoğlu, 1999; Çarpınlıoğlu and Gündoğdu, 2001; Özahi, 2011; Çarpınlıoğlu and Özahi, 2011, 2012, 2013).

LabView is a widely used visual programming language since 1986 (Whitley et al., 2006). It is designed to facilitate development of data acquisition, analysis, display and control applications. Unlike other text-based programs, LabView is a graphical program and based on the dataflow paradigm. Many common data processing or mathematical functions are already built-in and available such as spectral analysis, FFT approximation, etc. It is also possible for researchers to incorporate the algorithm into their existing or modified LabView programs. The program is consisted of functions which are called as virtual instruments (VIs). LabView VIs contain three main components such as *Front Panel*, *Block Diagram* and *Icon/Connector Pane*. *Front Panel* is an interface and used for specifying the inputs and outputs of the program. *Block Diagram* is related on an actual data flow between the inputs and the outputs, which is a source code of LabView program. *Icon/Connector Pane* graphically represents a virtual instrument (VI) in the block diagram and allows to use and to view a VI in another VI. Each VI also consists of three basic components of *terminals*, *nodes* and *wires*. *Terminals* may be input, output or constant values. *Nodes* are VI's operators, function calls and structure nodes. *Operators and function calls* are computations built into LabView and mathematical expressions. The examples of the *structure nodes* are *Flat Sequence Structure*, *Case Structure*, *For Loop* and *While Loop*. In LabView, data values travel on wires and pass through functions. Data flow is controlled by structures. *While Loop* and *For Loop* are structures that repeat the execution of a sub diagram. *Case Structure* is analogous to case If-Then-Else used in text-based programs. *Sequence Structure* executes diagrams sequentially in the order in which they appear (Beyon, 2001; Johnson, 1997; Wells, 1995, 1997).

In this paper, the functionality and the features of the devised program LabView 2009SP1® are verified introducing the sample plots of velocity and frictional field analyses. The devised program has also ability to analyze other types of time dependent and steady pipe flows besides pulsatile flow. The experimental setup and the used methodology within the devised program are presented in the following sections to show and verify the functionality, effectiveness and accuracy of the proposed program giving the results of the automatic test system.

EXPERIMENTAL SETUP

Pulsatile air flow through a smooth PVC pipeline of 26.6 mm diameter is generated by means of the devised program, *TDFC.vi* which triggers a mass flow control (MFC) unit which has a flow capacity between 0 and 0.003 m^3/s at an accuracy of ±1% at 4.5 bar (Çarpınlıoğlu and Özahi, 2011; Durst et al., 2003; Özahi and Çarpınlıoğlu, 2012; Çarpınlıoğlu and Özahi, 2012). The air flow through the MFC unit is supplied using a screw air compressor. The schematic layout and photography of the setup are given in Fig. 1.

A pair of flow conditioners which are placed at 12*D and* 14*D* downstream of the MFC unit are used in order to obtain fully developed flow in the pipe at feasible lengths, whose details are given in (Çarpınlıoğlu and Özahi, 2011). DANTEC 56C01 constant temperature anemometer (CTA) with a miniature hotwire probe, 55P11 whose in-situ calibration method is given in (Özahi and Çarpınlıoğlu, 2010), is used for the velocity measurements at X/D=604 where the laminar flow is fully developed. Local static pressures at 7 downstream locations of the pipeline (Fig. 1) are measured by WIKA SL-1 pressure transmitters having operating pressure ranges between -2000 kPa and 2000 kPa, response time of 1 ms and accuracy of <0.5 %. A 16-bit, 1-MHz A/D converter IOtech Daq3001 USB board connected to a PC is used for the control of the MFC unit, the velocity and pressure data acquisition with a sampling frequency of 100 Hz without any signal aliasing and excess data storage. The Daq3001 USB board is set to take 5000 data readings of local instantaneous velocity $U=U(r,t)$ and local instantaneous static pressures $P=P(t)$ (Çarpınlıoğlu and Özahi, 2013). Main characteristic parameters of pulsatile pipe flow such as Re_{ta}, Re_{os}, $\sqrt{\omega'}$ and A_1 are changed systematically by means of the devised program.

The program is utilized for the experimental study which has a capability of the analyses for a wide range of different $\sqrt{\omega'}$ and A_1 values in the ranges of $2.72\pm0.00 \le \sqrt{\omega'} \le 32.21\pm0.00$ and $0.05\pm0.0017 \le A_1 \le 0.96\pm0.03$, respectively. The experimental ranges of the case study are given in Table 1. The more details of the experimental study can be found in (Özahi, 2011). In Table 2, the results of the uncertainty analysis of the experimental study are given. The uncertainty analysis utilized for the velocity and pressure measurement is based on the well-known equation given in (ANSI/ASME PTC 19.1-1985; GUM, 2008; Holman, 2012; Coleman, 1989, Wheeler and Ganji, 1996). The detailed uncertainty analysis of the experimental study can be found in (Çarpınlıoğlu and Özahi, 2013).

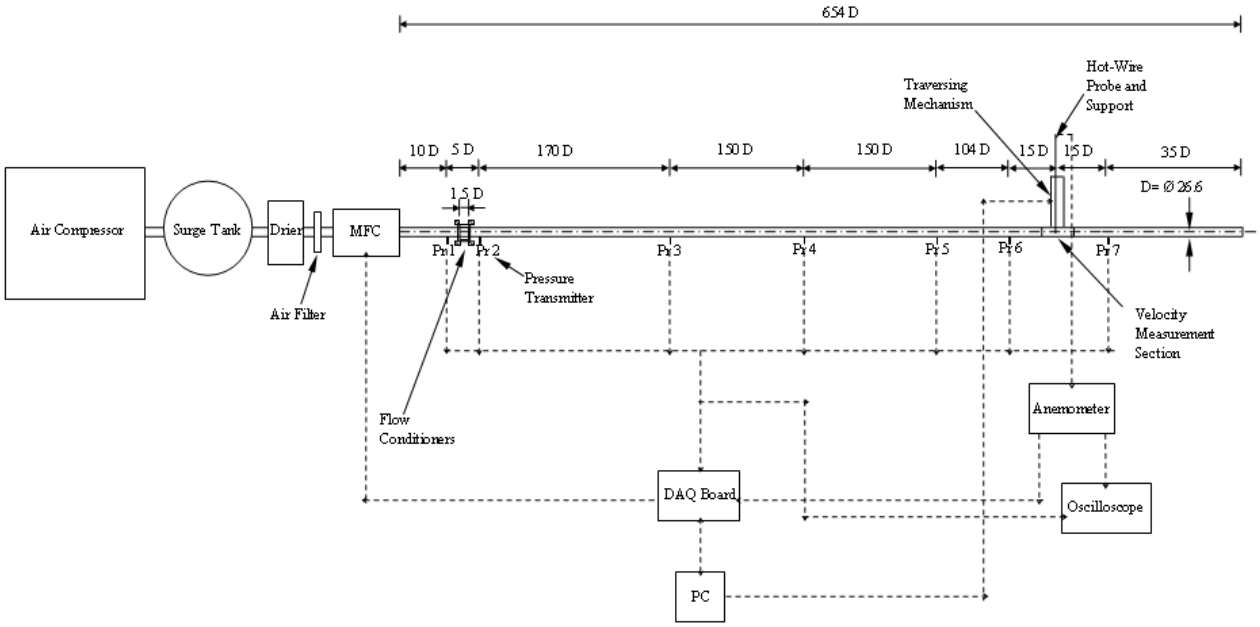

(a)

(b)

Figure 1. (a) Schematic layout of the experimental setup. (b) Photography of the experimental setup

Table 1. Experimental ranges

f (Hz)	$\sqrt{\omega'}$	A_1	Re_{ta}	Re_{os}
		$0.10 \leq A_1 \leq 0.96$	$2347 \leq Re_{ta} \leq 3133$	$272 \leq Re_{os} \leq 2248$
0.1	**2.72**	**0.47**	**2174**	**1029**
		0.53	**3018**	**1610**
0.2	3.85	$0.20 \leq A_1 \leq 0.90$	$2907 \leq Re_{ta} \leq 4817$	$572 \leq Re_{os} \leq 4261$
0.4	5.44	$0.21 \leq A_1 \leq 0.80$	$2150 \leq Re_{ta} \leq 4067$	$593 \leq Re_{os} \leq 2760$
0.6	6.67	$0.22 \leq A_1 \leq 0.86$	$1239 \leq Re_{ta} \leq 3330$	$583 \leq Re_{os} \leq 2862$
0.8	7.70	$0.32 \leq A_1 \leq 0.86$	$2307 \leq Re_{ta} \leq 3328$	$732 \leq Re_{os} \leq 2849$
1	8.61	$0.19 \leq A_1 \leq 0.90$	$1082 \leq Re_{ta} \leq 3157$	$521 \leq Re_{os} \leq 2748$
2	12.17	$0.29 \leq A_1 \leq 0.81$	$1390 \leq Re_{ta} \leq 2869$	$741 \leq Re_{os} \leq 2333$
4	17.22	$0.10 \leq A_1 \leq 0.90$	$1019 \leq Re_{ta} \leq 2662$	$277 \leq Re_{os} \leq 2339$
10	27.22	$0.12 \leq A_1 \leq 0.80$	$1294 \leq Re_{ta} \leq 3052$	$340 \leq Re_{os} \leq 2209$
14	32.21	$0.05 \leq A_1 \leq 0.74$	$1449 \leq Re_{ta} \leq 2877$	$137 \leq Re_{os} \leq 2121$

Table 2. Evaluated uncertainty values of the experimental study ranges

Measured/Evaluated Data in the Experiment	Unit	Overall Uncertainty (%)
$U(r,t)$	m/s	±3.2
$P(t)$	V	±0.8
	Pa	±1.3
$\bar{U}_{m,ta}$, $\lvert\bar{U}_{m,os.1}\rvert$	m/s	±3.4
Re_{ta}, Re_{os}	-	±3.4
$\Delta\bar{P}(t)/L$	Pa/m	±1.6
$\bar{\tau}_w(t)$	Pa	±1.9
$\lambda_u(t)$	-	±7.1

METHODOLOGY AND PROCESSING STYLE

The methodology and the process used in *TDFC.vi* are introduced in this section giving some details of the block diagram by means of the sample results generated after the evaluation procedures in LabView. The *functions* and *mathematical operators* to control the front panel objects are in the block diagram of the program. The other part is the front panel which is an interactive interface used by program users to generate steady or any form of time dependent signals, to control the MFC unit and to acquire data from the measurement devices. To meet the needs of the experimental study, the software program is designed in three major steps as can be seen from the software flow chart in Fig. 2. The first part of *TDFC.vi* is based on the flow generation and control. The controls are used to select the configuration of the flow type such as the type of daqboard, scan rate, total scan to acquire and to generate any steady or time-dependent pipe flows of any frequency in the range of 0.1 Hz≤*f*≤100 Hz, amplitude and offset value in the range of the MFC unit capacity. There are 3 segments labeled as *Analog Input*, *Analog Output* and *Voltage Output* as controls. As can be seen from Fig. 3a, *Analog Output* segment is used for generation and control of time dependent air flow for any type of waveforms in any ranges of oscillation frequency with any desired amplitude and mean values in the range of the MFC unit capacity. The voltage sent to the MFC unit between 0 and 10 V is corresponding to the flow rate values of 0 and 0.003 m^3/s. *Voltage Output* segment is used only for generation of steady flow. *Analog Input* segment is used to acquire the data from the hotwire anemometer and 7 pressure transmitters.

The second part of *TDFC.vi* is related with the data acquisition and measurement. In order to acquire the data from the hotwire anemometer and 7 pressure transmitters, *DAQIO READ SCAN.vi* is used in order to convert the digital value to the analog ones in the voltage unit. The third part of *TDFC.vi* is used for the processing and post-processing of the acquired data. The first part of the *Flat Sequence Structure* is used for the control of the MFC unit and for acquisition, processing and saving of data taken from the measurement devices. The second part is used for post-processing of the acquired data, i.e. for the evaluations of $\bar{U}_{m,ta}$, and $\lvert\bar{U}_{m,os.1}\rvert$ to process the raw velocity and pressure data, in the first step it is essential to separate all data from each other. For this reason, *Index Array* palette is used. Then raw velocity data in voltage are wired to *King's Law.vi* to convert them into the processed velocity data in unit of m/s. All other raw pressure data in voltage are wired to the *Pressure Transducers' Calibration.vi* for transformation of the raw pressure data into the processed ones in unit of Pa. As a result of *While Loop* execution, the continuous acquisition of raw velocity and pressure data are performed. After the velocity measurement and performing the statistical analyses at a radial position through the pipe cross section, the hotwire probe is positioned to the next radial location by means of the traverse mechanism. Then the velocity measurement with its statistical analyses is performed at new radial position by pressing the "NEXT STEP" button on the front panel. This procedure is repeated for 13 different radial positions through the half of pipe cross section without exiting from the program.

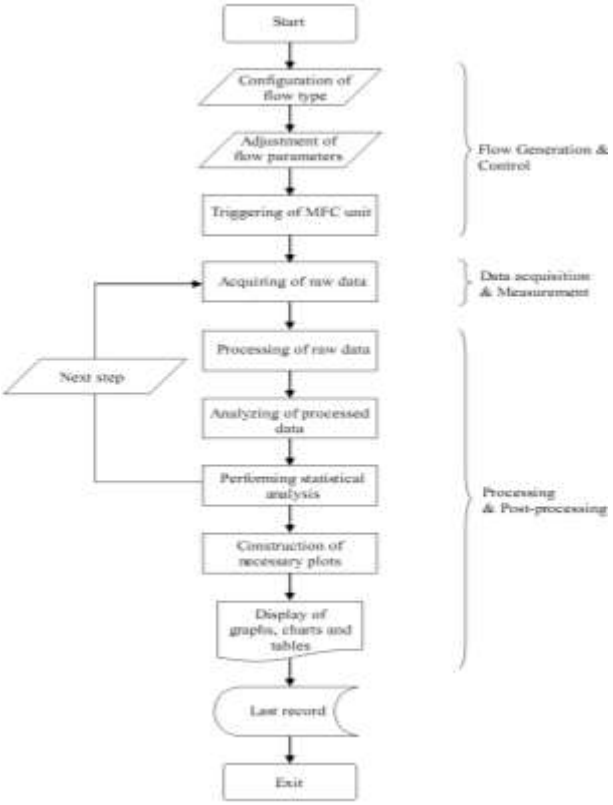

Figure 2. Flow chart of *TDFC.vi*.

On the front panel, there are also many indicators which show the results of the experimental data as numerical and graphical representations. The raw and processed velocity and pressure data are shown with these indicators. The instantaneous velocity and pressure waveforms can also be seen in the front panel by means of the *waveform charts* as can be seen from Fig. 3b. This part also executes for the calculations of Re_{ta}, Re_{os}, A_1, $\bar{\tau}_w(t)$, $\Delta\bar{P}(t)/L$, $\lambda_u(t)$, $\lambda_{u,ta}$, $\lambda_{qL}(t)$ and λ_{sL} and the other dimensionless parameters of S, ω', δ_S and $Re_{\delta s}$. Furthermore the necessary graphs, charts and tables are constructed as a result of post-processing the data in the third part of the program, then they are displayed on the front panel and saved into the predefined files in PC.

The whole analyses of the processed velocity and pressure data and their statistical analyses are performed in this part of the devised program. Lastly all processes during the execution of the program are saved in PC and the program is finalized by means of "END ACQUISITION" button.

RESULTS AND DISCUSSION

The results of *TDFC.vi* are given herein corresponding to two specified runs denoted with bold terms in Table 1. The first illustrated run at f=0.1 Hz ($\sqrt{\omega'}$ =2.72) belongs to the laminar regime in which Re_{ta} =2174, Re_{os} =1029 and A_1=0.47. The second run at f=0.1 Hz ($\sqrt{\omega'}$ =2.72) is related to the onset of transition to turbulence in which Re_{ta} =3018, Re_{os}=1610 and A_1=0.53.

The statistical measurements and FFT analysis of the data are carried out in the first section of the block diagram of *TDFC.vi*. The time-averaged and the oscillating component of velocity waveform, $\bar{U}_{ta}$ and $|\bar{U}_{os.1}|$ are evaluated for each radial position of the hotwire probe through the pipe cross section. The block diagram of this subvi is given in Fig. 4. The standard deviation, RMS value, skewness, range and FFT peak of 5000 velocity data are also evaluated in this subvi using the features of LabView environment. Besides this, the frequency of oscillation, f, is detected in the subvi. It is observed that the detected frequency of the velocity waveform is exactly the same as that sent to the MFC unit at the start of the program execution from the *Analog Output* segment.

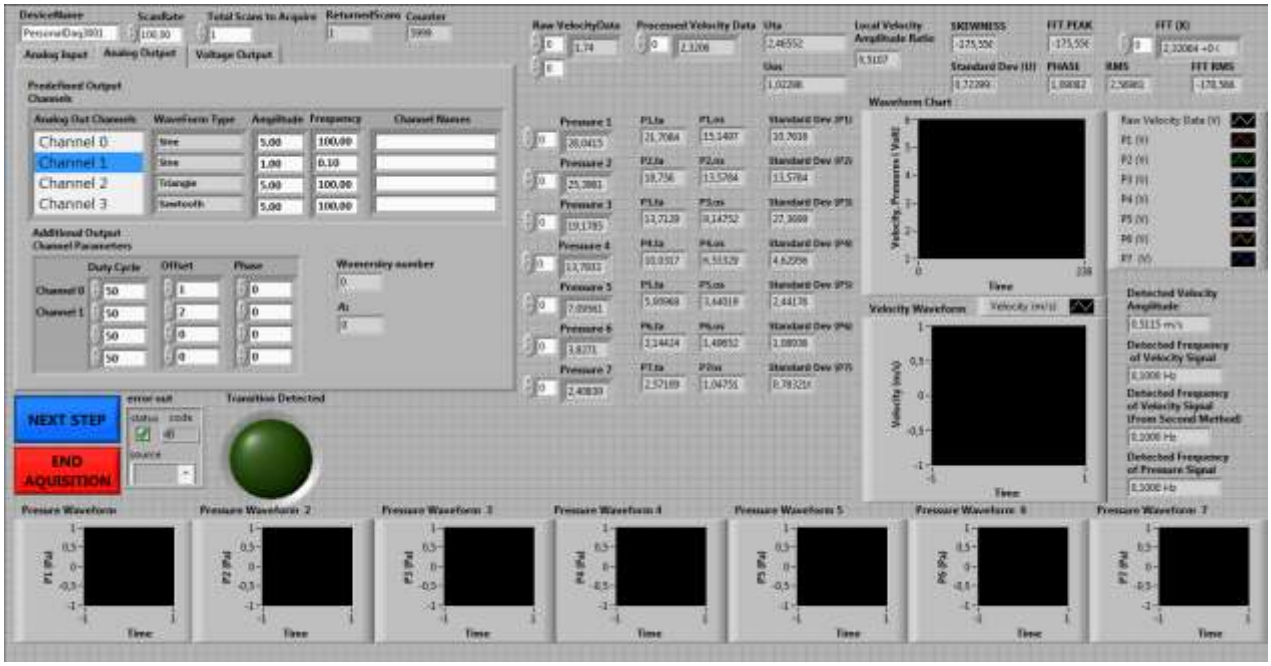

(a)

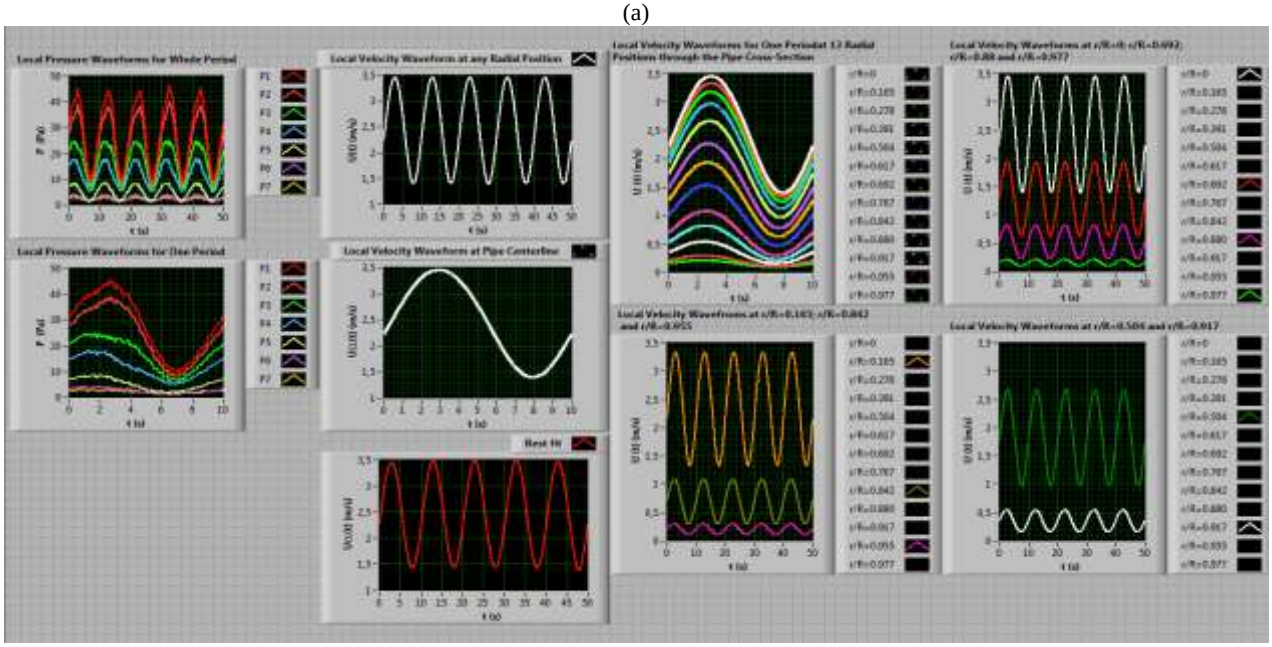

(b)

Figure 3. A part of the front panel of *TDFC.vi*: (a) *Analog Output* segment to control of MFC unit for generation of time-dependent flow. (b) Representations of pressure and velocity waveform graphs.

Figure 5 shows the velocity waveforms obtained from this subvi for each r/R position at Re_{ta}=2174, Re_{os}=1029, A_1=0.47 and $\sqrt{\omega'}$ =2.72. No turbulent structure is seen on these velocity waveforms in Fig. 5 while laminar to turbulent transition is seen at all r/R positions (Fig. 6) at Re_{ta}=3018, Re_{os} =1610, $\sqrt{\omega'}$ =2.72 and A_1=0.53. As can be seen from Fig. 6, the transition to turbulence starts at the end of the decelerating phase of the waveform and then the relaminarization occurs during the accelerating and at the beginning of the decelerating phases, which is the same with the observed structures in the papers of (Iguchi and Ohmi, 1982; Shemer, 1985; Stettler and Hussain, 1986; Özahi and Çarpınlıoğlu, 2013).

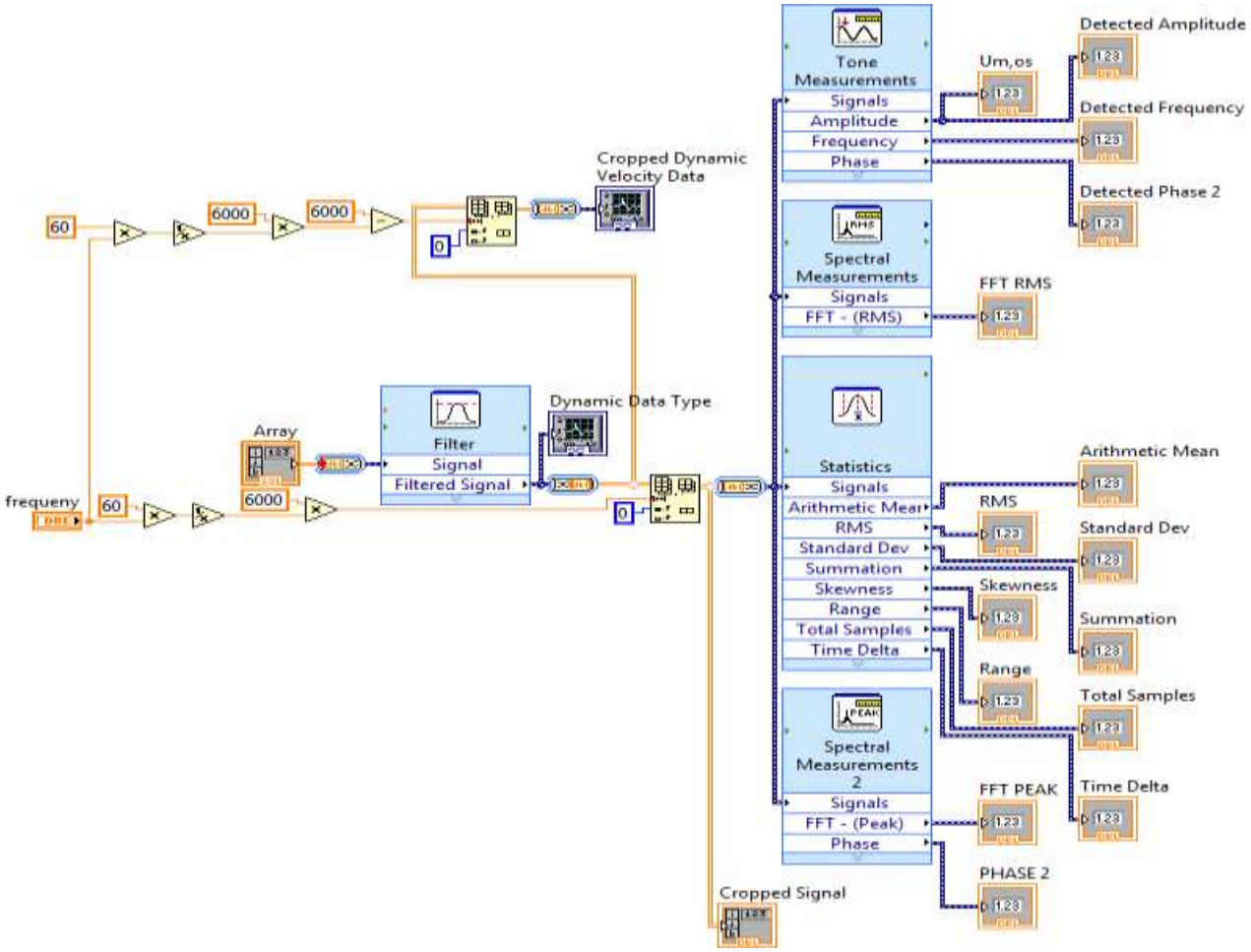

Figure 4. Sub-block diagram of *Statistics of Velocity.vi* for the statistical measurements and FFT analysis of the velocity data.

Fig. 7 shows the velocity waveforms acquired by means of *TDFC.vi* at r/R=0.977 and r/R=0. As is seen, the onset of transition begins always at the same locations illustrated on the graphs.

In order to acquire and process the velocity data at each radial position of the traversed hotwire probe, the *Case Structure* is used for 13 times without exiting from the main program, clicking on the "NEXT STEP" button on the front panel. The static pressure data which are taken for 13 times in a run are found to be the same with an accuracy of ±0.8% at each pressure transmitter's location during the accumulation of the velocity data for 13 radial positions.

$\overline{U}_{ta}$ and $\left|\overline{U}_{os,1}\right|$ data evaluated for each radial position of the hotwire probe are used in order to obtain the cross sectional $\overline{U}_{ta}$ and $\left|\overline{U}_{os,1}\right|$ distributions with respect to the radial position, r, respectively by means of *Replace Array Subset* palettes. In order to calculate the time averaged and oscillating component of the mean velocity through the pipe cross section, $\overline{U}_{m,ta}$ and $\left|\overline{U}_{m,os,1}\right|$, respectively, two different methods are used in the program. In the first method, each time averaged and oscillating component of velocity, $\overline{U}_{ta}$ and $\left|\overline{U}_{os,1}\right|$ are evaluated at each radial position of the hotwire probe through the cross-section of the pipe as is seen in the front panel of *TDFC.vi* in Fig. 8. $\overline{U}_{ta}$ and $\left|\overline{U}_{os,1}\right|$ distributions are then plotted separately with respect to the corresponding radial positions and curve fittings are applied for both $\overline{U}_{ta}$ and $\left|\overline{U}_{os,1}\right|$ distributions. This evaluation method is the novel one which contributes a new insight to the literature. Fig. 9 shows the distributions of $\overline{U}_{ta}$ and $\left|\overline{U}_{os,1}\right|$ obtained by means of the program for the sample runs.

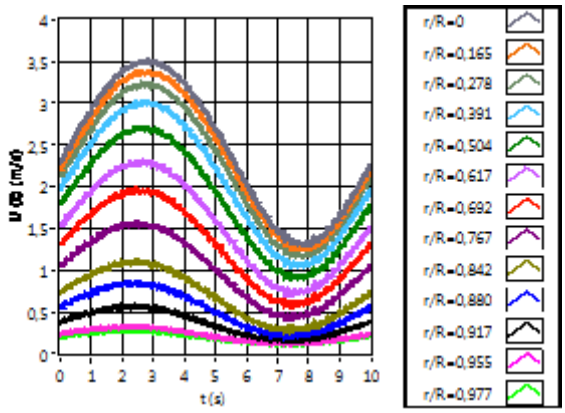

Figure 5. One-period velocity waveforms for different r/R positions at Re_{ta} =2174, Re_{os} =1029, $\sqrt{\omega'}$ =2.72 and A_1=0.47.

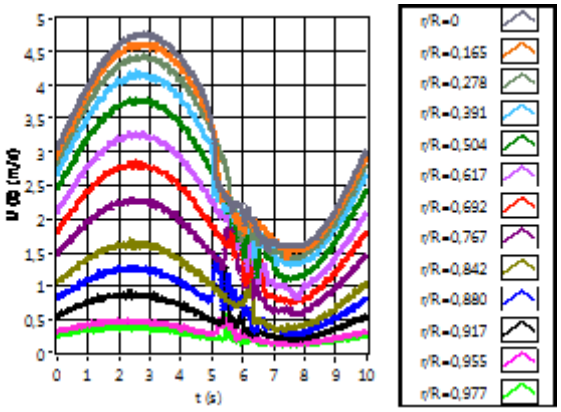

Figure 6. One-period velocity waveforms for different r/R positions at Re_{ta} =3018, Re_{os} =1610, $\sqrt{\omega'}$ =2.72 and A_1=0.53.

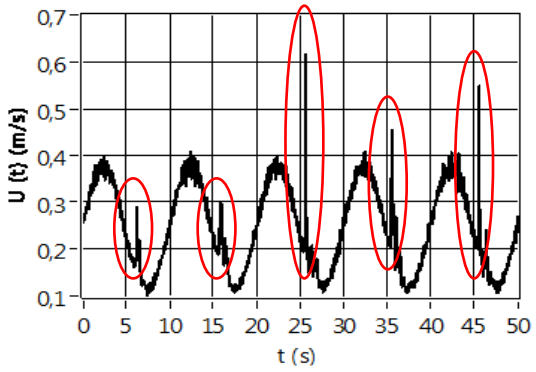

(a) r/R=0.977

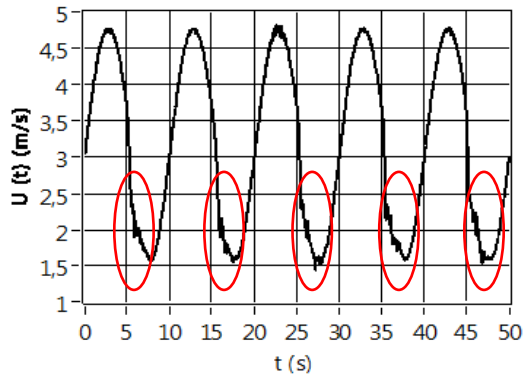

(b) r/R=0

Figure 7. Velocity waveforms near the pipe wall and at the pipe centerline at Re_{ta} =3018, Re_{os} =1610, $\sqrt{\omega'}$ =2.72 and A_1=0.53.

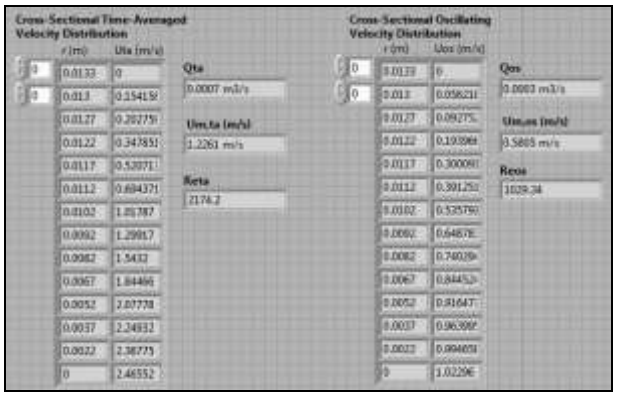

Figure 8. A part of the front panel corresponding to the cross sectional time averaged and oscillating velocity distributions with respect to the radial positions.

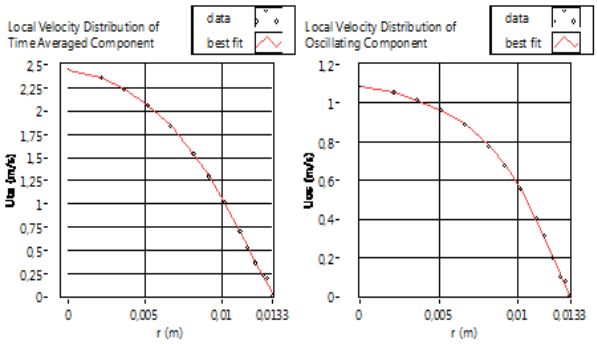

(a) Re_{ta} =2174, Re_{os} =1029, $\sqrt{\omega'}$ =2.72

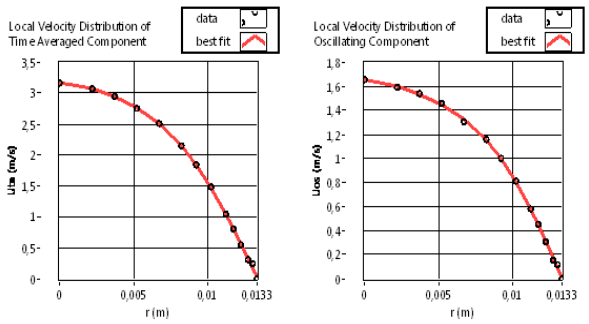

(b) Re_{ta} =3018, Re_{os} =1610, $\sqrt{\omega'}$ =2.72

Figure 9. Cross sectional velocity distributions of time averaged and oscillating components developed by *TDFC.vi*

These velocity distributions are later used for estimation of $\overline{U}_{m,ta}$, $\left|\overline{U}_{m,os,1}\right|$, Re_{ta} and Re_{os} (see Fig. 8). Hence Re_{ta} and Re_{os} are calculated in the same subvi. The velocity amplitude ratio, A_1, is also evaluated by the definition of $A_1 = \left|\overline{U}_{m,os,1}\right| / \overline{U}_{m,ta}$ for each run.

In the *Second Method*, the $\overline{U}(t)$ values of the cycle for each phase at 13 different radial positions of the pipe are firstly saved as a matrix form and the cross sectional mean velocity, $\overline{U}_m(t)$, for each phase of the cycle are evaluated by numerically integrating the ensemble averaged data over the cross section of the pipe by using the well-known Sympson's rule in the program. Then the

evaluated $\overline{U}_m(t)$ is approximated in the program by the finite Fourier series expansion using Eq. (2). Using the *Second Method*, $\overline{U}_{m,ta}$ and $|\overline{U}_{m,os,1}|$ and f values are then determined in *Second Method.vi*. These values are then compared with those obtained using the first method and a good conformity is found with ± 0.2% mean deviation for $\overline{U}_{m,ta}$, ± 1.1% mean deviation for $|\overline{U}_{m,os,1}|$ and ± 0% mean deviation for f. All evaluated values of flow parameters using both *First* and *Second Method* are saved into the corresponding file. All waveform graphs and charts plotted in both first and second part of *Flat Sequence Structure* are saved into the file using the subvis of *Waveform Graphs and Charts.vi* and *Waveform Graphs and Charts.vi*. *Export Image* as an *Invoke Node* is used for this purpose.

The non-dimensional velocity distributions of the time averaged and the oscillating components in the laminar regime and at the onset of transition are given in Figs. 10 and 11, respectively for the sample illustrations acquired from each value of $\sqrt{\omega'}$.

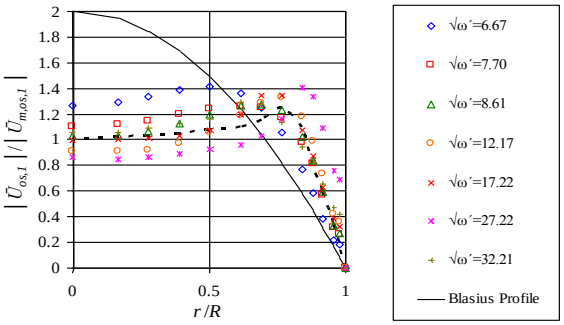

(b)

Figure 10. Non-dimensional velocity distributions of time averaged and oscillating components in the laminar regime.

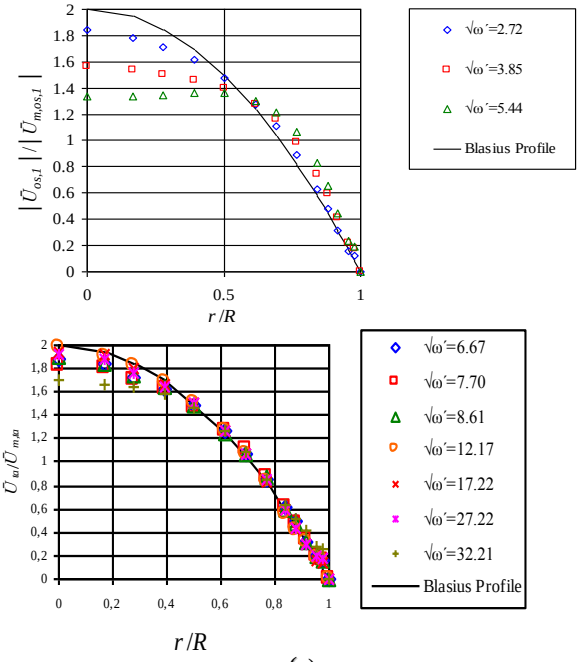

(a)

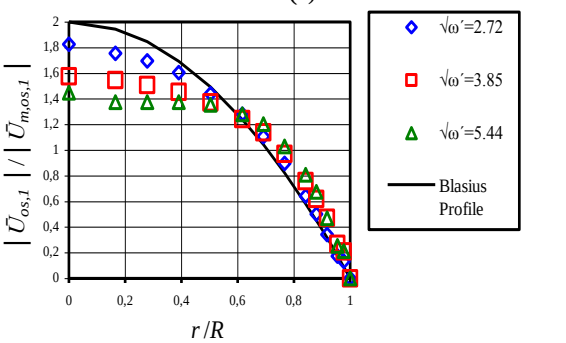

(b)

Figure 11. Non-dimensional velocity distributions of time averaged and oscillating components at the onset of transition.

The distribution of $\overline{U}_{ta}/\overline{U}_{m,ta}$ in the pulsatile laminar flow is parabolic in shape obeying to the well-known Blasius profile for that in the steady laminar regime (Fig. 10a), however there is a deviation from the Blasius profile at the onset of transition (Fig. 11a). The profiles of $|\overline{U}_{os,1}|/|\overline{U}_{m,os,1}|$ are rather different than the usual steady laminar profiles (Figs. 10b and 11b). As is seen from the figures, $|\overline{U}_{os,1}|/|\overline{U}_{m,os,1}|$ distribution is compatible with theoretical laminar theory for $|\overline{U}_{os,1}|$, Eq. (7), which is given in the paper of Ohmi et al. (1982).

$$|\overline{U}_{os,1}| = \frac{1}{\rho_0 \omega}\frac{|\Delta\overline{P}_{os,1}|}{L}\times \frac{}{\sqrt{1+\left\{\frac{M_0\left(r'\sqrt{\omega'}\right)}{M_0\left(\sqrt{\omega'}\right)}\right\}^2 - 2\frac{M_0\left(r'\sqrt{\omega'}\right)}{M_0\left(\sqrt{\omega'}\right)}\cos\left\{\theta_0\left(r'\sqrt{\omega'}\right)-\theta_0\left(\sqrt{\omega'}\right)\right\}}} \quad (7)$$

Besides the velocity field analyses, the pressure waveforms are also analyzed by means of *TDFC.vi*. The one-period pressure waveforms for both runs are illustrated in Fig. 12. The pressure waveforms in Fig. 12a are seen to be sinusoidal and their magnitudes tend to decrease at downstream locations of the pipeline. However, the pressure waveforms which belong to the transitional regime in Fig. 12b are not seen to be regular although it is in sinusoidal shape. There are some swashes on the waveform due to flow being transitional.

The time averaged and the oscillating components of the pressure waveform, $\overline{P}_{ta}$ and $|\overline{P}_{os,1}|$ are evaluated in *Tone Meas. of Pressures.vi* whose block diagrams are shown in Fig. 13 for all pressure data acquired from 7 pressure transmitters. The standard deviations of the pressure data are also evaluated using *Statistics of Pressure.vi*.

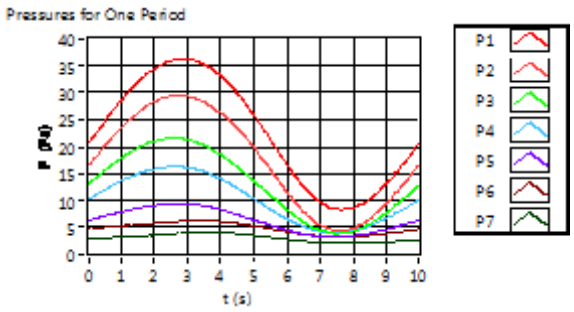

(a) Re_{ta} =2174, Re_{os} =1029, $\sqrt{\omega'}$ =2.72

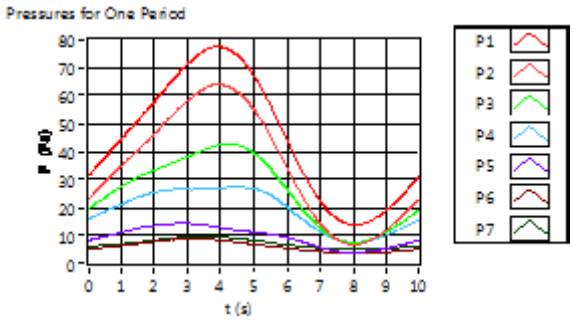

(b) Re_{ta} =3018, Re_{os} =1610, $\sqrt{\omega'}$ =2.72

Figure 12. Pressure waveforms acquired at each downstream locations (a) in the laminar regime and b) at the onset of transition.

The frequencies of the pressure waveforms are detected using the *Frequency and Amplitude Detection of Pressure Signal.vi*. The frequencies of the pressure waveforms are found to be the same as those of the velocity waveforms. *Pressure Drop Determination.vi* is used for calculation of the pressure drop per unit length at the test section, $\Delta\overline{P}(t)/L = (\overline{P}_6 - \overline{P}_7)/L$. The time averaged and the oscillating components of pressure drop per unit length, $\Delta\overline{P}_{ta}/L$ and $|\Delta\overline{P}_{os,1}|/L$ are also evaluated in this subvi. All $P(t)$, $\overline{P}_{ta}$, $|\overline{P}_{os,1}|$, $\Delta\overline{P}_{ta}/L$ and $|\Delta\overline{P}_{os,1}|/L$ evaluated are saved into the file using *Saving of Instantaneous All Data.vi* and *Saving of Instantaneous Pressure Data.vi*.

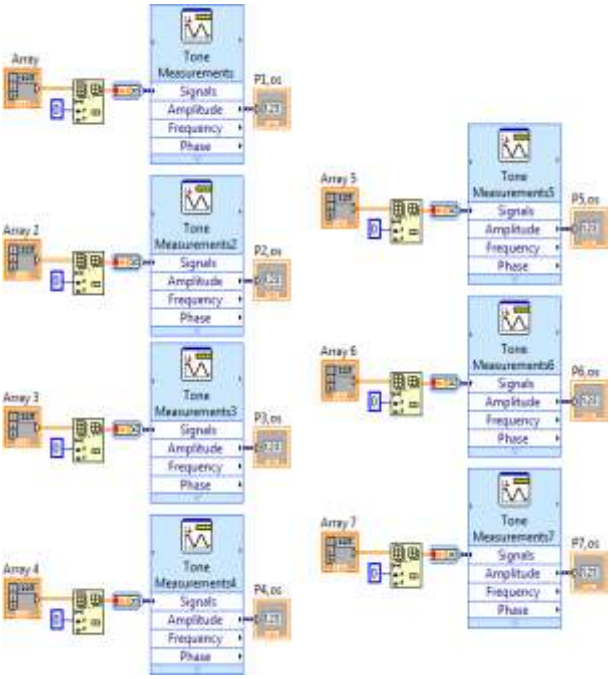

Figure 13. Sub-block diagram of *Tone Meas. of Pressures.vi* for the statistical analysis of the pressure data.

The theoretical mean velocity distribution, $\overline{U}_m(t)$ is expressed by means of Eq. (2) using $\overline{U}_{m,ta}$ and $|\overline{U}_{m,os,1}|$. The theoretical $\Delta\overline{P}(t)/L$ is also expressed using the evaluated values of $\Delta\overline{P}_{ta}/L$ and $|\Delta\overline{P}_{os,1}|/L$ using the following equation;

$$\Delta\overline{P}(t)/L = \Delta\overline{P}_{ta}/L + (|\Delta\overline{P}_{os,1}|/L)\sin(\omega t + \angle\Delta\overline{P}_{os,1}) \quad (8)$$

TDFC.vi evaluates also the instantaneous wall shear stress, $\overline{\tau}_w(t)$ in *Wall Shear Stress.vi* using the experimental data of $\overline{U}_m(t)$ and $\Delta\overline{P}(t)/L$ in the time dependent momentum integral equation (Eq. (3)) and plots the instantaneous profiles of $\overline{U}_m(t)$, $\Delta\overline{P}(t)/L$ with their FFT approximations and $\overline{\tau}_w(t)$ in the same graph. The one-period variations of $\overline{U}_m(t)$, $\Delta\overline{P}(t)/L$ with their FFT approximations and $\overline{\tau}_w(t)$ for both runs are given in Fig. 14. As is seen in Fig. 14a, there are good conformity with the experimental data and their FFT

approximations for both $\overline{U}_m(t)$ and $\Delta\overline{P}/L(t)$ for Re_{ta}=2174, Re_{os}=1029, $\sqrt{\omega'}$ =2.72 and A_1 =0.47 with mean deviations of ±1.5% and ±3%, respectively, due to the flow being laminar. However, when laminar to turbulent transition occurs, as can be seen for the run at Re_{ta}=3018, Re_{os} =1610, $\sqrt{\omega'}$ =2.72 and A_1 =0.53, the deviations between the experimental data and their FFT approximations of $\overline{U}_m(t)$ and $\Delta\overline{P}/L(t)$ are observed (Fig. 14b).

Furthermore, $\lambda_u(t)$, $\lambda_{u,ta}$ and $\lambda_{qL}(t)$ are calculated and the results are plotted in the waveform graphs in *Friction Factors.vi* of *TDFC.vi*. The variations of $\lambda_u(t)$ and $\lambda_{qL}(t)$ which are for time dependent and quasi steady flows, respectively, are seen together for both runs in Fig. 15. There are big differences between these two types of friction factors because the flow is neither steady nor quasi steady.

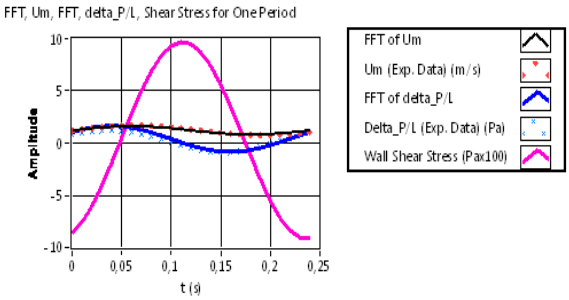

(a) Re_{ta} =2174, Re_{os} =1029, $\sqrt{\omega'}$ =2.72

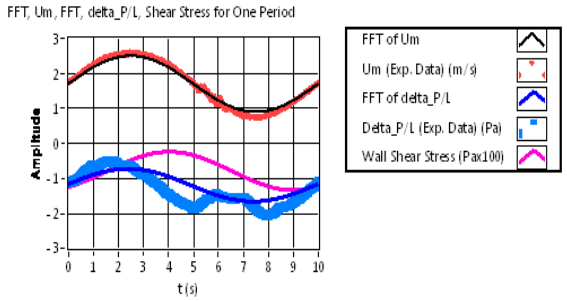

(b) Re_{ta} =3018, Re_{os} =1610, $\sqrt{\omega'}$ =2.72

Figure 14. Combined graphical representations of $\overline{U}_m(t)$, $\Delta\overline{P}/L(t)$ with their FFT approximations and $\overline{\tau}_w(t)$ in the laminar regime and at the onset of transition.

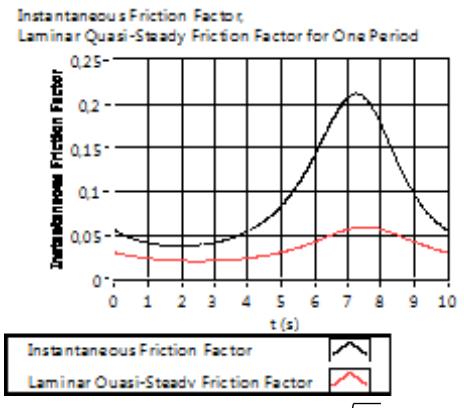

(a) Re_{ta} =2174, Re_{os} =1029, $\sqrt{\omega'}$ =2.72

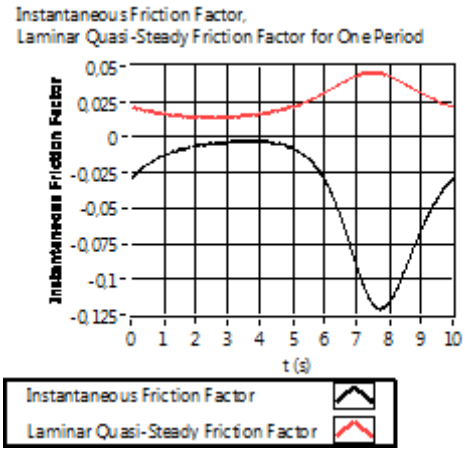

(b) Re_{ta} =3018, Re_{os} =1610, $\sqrt{\omega'}$ =2.72

Figure 15. Comparisons of $\lambda_u(t)$ and $\lambda_{qL}(t)$ in the laminar regime and at the onset of transition.

Besides the inevitable features of *TDFC.vi* as generation, control, data acquisition and processing of both steady and time dependent pipe flows, *TDFC.vi* has also ability to detect automatically onset of transition (Özahi and Çarpınlıoğlu, 2013). In order to detect the onset of transition to turbulence in the flow, the first derivative of $U(r,t)$ is taken at each radial position of the hotwire probe as a preliminary process of the turbulence detection method. The turbulence detection method is devised differently for low frequency (f≤1 Hz) and high frequency (f >1 Hz) ranges because f=1 Hz has been found to be the critical point which is declared in the paper of (Çarpınlıoğlu and Özahi, 2012). The detection method is based on the comparison of the defined turbulence detection parameter (TDP) and threshold parameter (TP). If TDP is greater than TP, the subprogram detects the onset of transition. The detection of the onset of transition is performed by means of true or false cases as can be seen from Fig. 16. For f≤1 Hz, the true case structure begins to run for the detection of transition if it exists. If f >1 Hz, the false structure in which there are different functions of TDP and TP than those for f≤1 Hz executes. If the transition is detected at any time of the velocity waveform and any radial positions of the hotwire probe, the green lamp lights and it gives an alert on the front panel.

CONCLUSION

TDFC.vi which has been devised in LabView 2009SP1® environment for generation, control, data acquisition and processing in pulsatile pipe flow is presented in this paper giving the front panel and block diagrams of *TDFC.vi* and introducing some related graphical representations about the working principles of the program.

Some concluding remarks are outlined as follows:

1) The presented data and graphs for two specified runs illustrate the applicability and functionality of *TDFC.vi* for both laminar and transitional regimes.

2) All difficulties and weary processes to process and analyze the data are eliminated and time can be saved by means of the devised program.

3) More accurate and precision measurements and analyses are handled by means of the automatically controlled program without any human error.

4) The results obtained in the program ensure relatively high velocity and pressure measurement chains in the 6) With the aid of the devised program, it becomes easier to generate steady and/or time dependent flow at any desired oscillation frequency, amplitude and mean value of any types of waveforms, and more practical to process, analyze and plot of flow dynamical parameters.

7) By means of a little change in the devised program, it can be applicable for all other real-world studies in steady and/or time dependent pipe flow measurements.

8) The devised program and the used methodology contribute to the literature as an original insight such that accuracy with the uncertainties of ±3.2% and ±1.3%, respectively.

5) The devised program has an ability (i) to trigger the MFC unit and control the measurement devices, (ii) to acquire the data from the measurement devices, (iii) to process, analyze and post-process the data, (iv) to plot the necessary charts and graphs and (v) to save all data and their corresponding numerical and graphical results.

the devised program with the used methodology are convenient for other research studies in the future and for the educational purposes providing many advantages for the real laboratory studies with real instruments in the velocity and pressure measurements for not only time dependent but also steady flows.

9) The program gives a novel contribution in terms of the algorithm used for flow generation, control, data acquisition and processing giving an engineering relevance.

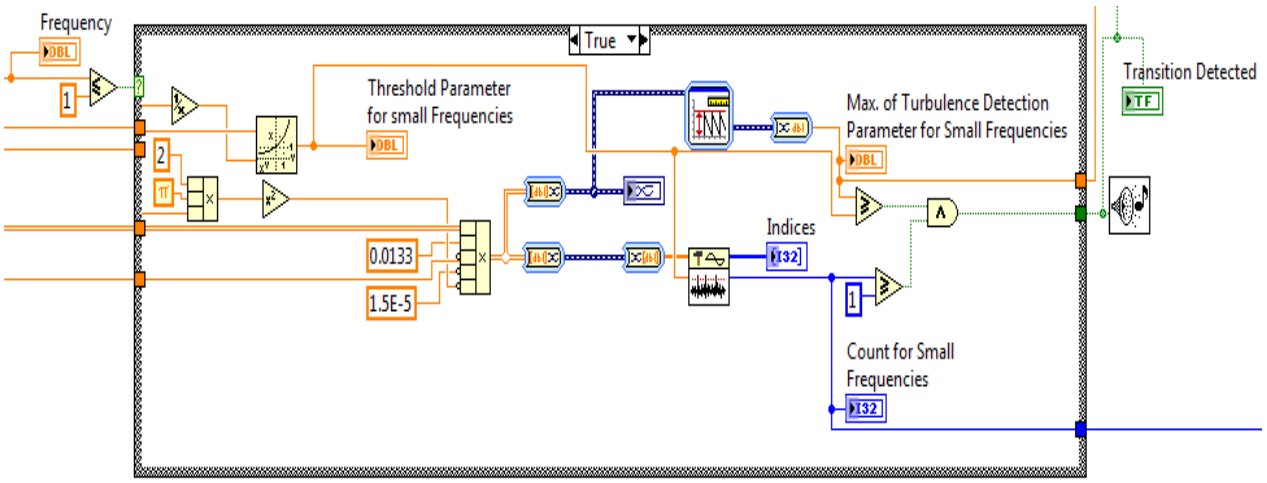

(a)

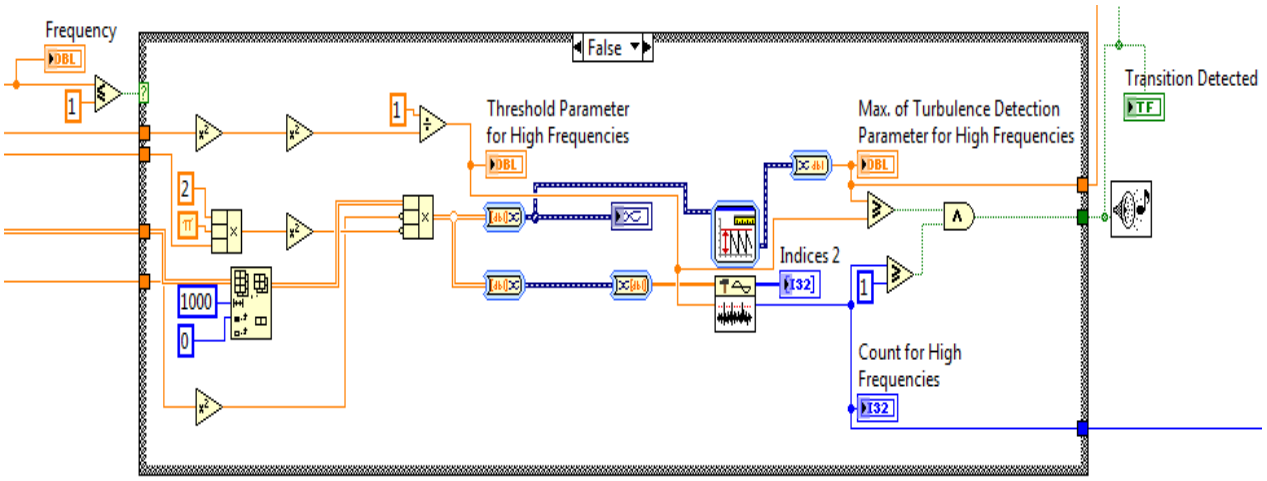

(b)

Figure 16. Sub-block diagram for the detection of laminar to turbulent transition for (a) $f \leq 1$ Hz and (b) $f > 1$ Hz.

REFERENCES

ANSI/ASME PTC 19.1-1985 Part 1, 1986, *Measurement Uncertainty* (Available from ASME Order Dept., 22 Law Drive, Box 2300, Fairfield, New Jersey 07007-2300).

Beyon J. Y., 2001, *LabView Programming, Data Acquisition and Analysis*, Prentice Hall, New York.

Coleman H. W. and Steele W. G. Jr., 1989, *Experimentation and Uncertainty Analysis for Engineers*, Wiley, New York.

Çarpınlıoğlu M. Ö. and Gündoğdu M. Y., 2001, A Critical Review on Pulsatile Pipe Flow Studies Directing Towards Future Research Topics, *Flow Meas. Instrum.*, 12, 163-174.

Çarpınlıoğlu M. Ö. and Özahi E., 2011, Laminar Flow Control via Utilization of Pipe Entrance Inserts (A Comment on Entrance Length Concept), *Flow Meas. Instrum.*, 22, 165-174.

Çarpınlıoğlu M. Ö. and Özahi E., 2012, An Updated Portrait of Transition to Turbulence in Laminar Pipe Flows with Periodic Time Dependence (A Correlation Study), *Flow Turbul. Combust.*, 89, 691-711.

Çarpınlıoğlu M. Ö. and Özahi E., 2012, An Experimental Research Project on Sinusoidal Pulsatile Pipe Flows Part 2: Influence of Oscillation Frequency and Amplitude on Onset of Transition to Turbulenc, *Proc. of the 3rd International Conference on Fluid Mechanics and Heat and Mass Transfer (Fluids-Heat'12)*, Athens, 45-50.

Çarpınlıoğlu M. Ö. and Özahi E., 2013, An Experimental Test System for the Generation, Control and Analysis of Sinusoidal Pulsatile Pipe Flows (An Application Case for Time Dependent Flow Measurements), *Flow Meas. Instrum.*, 32, 27-34.

Durst F., Heim U., Ünsal B. and Kullik G., 2003, Mass Flow Rate Control System for Time-Dependent Laminar and Turbulent Flow Investigations, *Meas. Sci. Technol.*, 14, 893-902.

Gündoğdu M. Y. and Çarpınlıoğlu M. Ö., 1999, Present State of Art on Pulsatile Flow Theory Part 1: Laminar and Transitional Flow Regimes, *JSME Int. J. Series B Fluids and Therm. Eng.*, 42, 384-397.

Holman J. P., 2012, *Experimental Methods for Engineers*, (8th Ed.), McGraw Hill, New York.

Iguchi M. and Ohmi M., 1982, Transition to Turbulence in a Pulsatile Pipe Flow Part 2: Characteristics of Reversing Flow Accompanied by Relaminarization, *Bull. JSME*, 25, 1529.

Johnson G.W., 1997, *Labview Graphical Programming: Practical Applications in Instrumentation and Control*, McGraw-Hill, New York.

Joint Committee for Guides in Metrology, Evaluation of measurement data-guide to the expression of uncertainty in measurement (GUM), JCGM 100, 2008.

Mizushina T., Maruyama T. and Shiozaki Y., 1973, Pulsating Turbulent Flow in a Tube, *J. Chem. Eng Jpn*, 6, 487-494.

Ohmi M. and Iguchi M., 1980, Flow Pattern and Frictional Losses in Pulsating Pipe Flow Part 2, Effect of Pulsating Frequency on the Turbulent Frictional Losses, *Bull. JSME*, 23, 2021-2028.

Ohmi M. and Iguchi M., 1981, Flow Pattern and Frictional Losses in Pulsating Pipe Flow Part 4 General Representation of Turbulent Frictional Losses, *Bull. JSME*, 24, 67-74.

Ohmi M. and Iguchi M., 1981, Flow Pattern and Frictional Losses in Pulsating Pipe Flow Part 6 Frictional Losses in a Laminar Flow, *Bull. JSME*, 24, 1756-1763.

Ohmi M., Iguchi M. and Urahata I., 1982, Transition to Turbulence in a Pulsatile Pipe Flow Part 1: Wave Forms and Distribution of Pulsatile Velocities Near Transition Region, *Bull. JSME*, 25, 182-189.

Özahi E., 2011, *Analysis of Laminar-Turbulent Transition in Time-Dependent Pipe Flows*, Ph.D. thesis, University of Gaziantep, Gaziantep, Turkey.

Özahi E. and Çarpınlıoğlu M. Ö., 2012, An Experimental Research Project on Sinusoidal Pulsatile Pipe Flows Part 1: Presentation of Software Programming Utilized for Measurements and Data Acquisition, *Proc. of the 3rd International Conference on Fluid Mechanics and Heat and Mass Transfer (Fluids-Heat'12)*, Athens, 39-44.

Özahi E. and Çarpınlıoğlu M. Ö., 2013, Determination of Transition Onset in Laminar Pulsatile Pipe Flows, *J. Therm. Sci. Tech.*, 33, 125-133.

Özahi E., Çarpınlıoğlu M. Ö. and Gündoğdu M. Y., 2010, Simple Methods for Low Speed Calibration of Hot-Wire Anemometers, *Flow Meas. Instrum*., 21, 166-170.

Shemer L., 1985, Laminar-Turbulent Transition in a Slowly Pulsating Pipe Flow, *Phys. Fluid*, 28, 3506-3509.

Stettler J. C. and Hussain K. M. F., 1986, On Transition of the Pulsatile Pipe Flow, *J. Fluid Mech.*, 170, 169-197.

Wells L. K., 1995, *LabView Student Edition User's Guide*, Prentice Hall, Englewood Cliffs NJ.

Wells L. K. and Travis J., 1997, *Labview for Everyone: Graphical Programming Made Even Easier*, Prentice Hall, Upper Saddle River NJ.

Wheeler A. J. and Ganji A. R., 1996, *Introduction to Engineering Experimentation*, Prentice Hall, New Jersey.

Whitley K. N., Novick L. R. and Fisher D., 2006, Evidence in Favor of Visual Representation for the Dataflow Paradigm: An Experiment Testing Labview's Comprehensibility, *Int. J. Human-Computer Studies*, 64, 281-303.

ACKNOWLEDGEMENTS

The authors would like to thank the Research Fund of the University of Gaziantep for the research project supported under grant no: MF.09.09 and RM.13.01.